Swiss J Geosci (2011) 104:285–298
DOI 10.1007/s00015-011-0060-6

Tracing metamorphism, exhumation and topographic evolution in orogenic belts by multiple thermochronology: a case study from the Nízke Tatry Mts., Western Carpathians

Martin Danišík · Jaroslav Kadlec · Christoph Glotzbach · Anett Weisheit · István Dunkl · Milan Kohút · Noreen J. Evans · Monika Orvošová · Brad J. McDonald

Received: 26 August 2010 / Accepted: 20 March 2011 / Published online: 27 May 2011

Abstract A combination of four thermochronometers [zircon fission track (ZFT), zircon (U–Th)/He (ZHe), apatite fission track (AFT) and apatite (U–Th–[Sm])/He (AHe) dating methods] applied to a valley to ridge transect is used to resolve the issues of metamorphic, exhumation and topographic evolution of the Nízke Tatry Mts. in the Western Carpathians. The ZFT ages of 132.1 ± 8.3, 155.1 ± 12.9, 146.8 ± 8.6 and 144.9 ± 11.0 Ma show that Variscan crystalline basement of the Nízke Tatry Mts. was heated to temperatures >210°C during the Mesozoic and experienced a low-grade Alpine metamorphic overprint. ZHe and AFT ages, clustering at ~55–40 and ~45–40 Ma, respectively, revealed a rapid Eocene cooling event, documenting erosional and/or tectonic exhumation related to the collapse of the Carpathian orogenic wedge. This is the first evidence that exhumation of crystalline cores in the Western Carpathians took place in the Eocene and not in the Cretaceous as traditionally believed. Bimodal AFT length distributions, Early Miocene AHe ages and thermal modelling results suggest that the samples were heated to temperatures of ~55–90°C during Oligocene–Miocene times. This thermal event may be related either to the Oligocene/Miocene sedimentary burial, or Miocene magmatic activity and increased heat flow. This finding supports the concept of thermal instability of the Carpathian crystalline bodies during the post-Eocene period.

Editorial handling: A.G. Milnes.

M. Danišík · N. J. Evans · B. J. McDonald
John de Laeter Centre of Mass Spectrometry,
Applied Geology, Curtin University of Technology,
GPO Box U1987, Perth, WA 6845, Australia

N. J. Evans · B. J. McDonald
CSIRO Earth Science and Resource Engineering,
ARRC, 26 Dick Perry Avenue, Kensington,
WA 6151, Australia
e-mail: Noreen.Evans@csiro.au

B. J. McDonald
e-mail: Brad.McDonald@csiro.au

M. Danišík (✉)
Department of Earth and Ocean Sciences, Faculty of Science and Engineering, The University of Waikato, Private Bag 3105,
Hamilton 3240, New Zealand
e-mail: M.Danisik@waikato.ac.nz

J. Kadlec
Institute of Geology, v.v.i., The Academy of Sciences
of the Czech Republic, Rozvojová 269, 16500 Prague 6,
Czech Republic
e-mail: kadlec@gli.cas.cz

C. Glotzbach
Institute of Geology, Leibniz University Hannover,
Callinstraße 30, 30167 Hannover, Germany
e-mail: glotzbach@geowi.uni-hannover.de

A. Weisheit
Institute of Geosciences, University of Tübingen,
Sigwartstraße 10, 72076 Tübingen, Germany
e-mail: anett.weisheit@uni-tuebingen.de

I. Dunkl
Geoscience Center Göttingen, Sedimentology and
Environmental Geology, Goldschmidtstrasse 3,
37077 Göttingen, Germany
e-mail: istvan.dunkl@geo.uni-goettingen.de

M. Kohút
Dionýz Štúr State Institute of Geology, Mlynská dolina 1,
817 04 Bratislava, Slovak Republic
e-mail: milan.kohut@geology.sk

M. Orvošová
The Slovak Museum of Nature Protection and Speleology,
Školská 4, 031 01 Liptovský Mikuláš, Slovak Republic
e-mail: orvosova@smopaj.sk

Keywords Exhumation · Zircon · Apatite · (U–Th–[Sm])/He dating · Fission track dating · Nízke Tatry Mts. · Western Carpathians · Thermal modelling

1 Introduction

The Western Carpathians in central Europe represent the northernmost branch of the Alps and form the westernmost segment of a curved Carpathian orogenic belt (Fig. 1a). Similarly to other sectors of the Alpine belt, the Western Carpathians have experienced a rather complex Alpine tectonothermal history, comprising Jurassic rifting and basin formation, Cretaceous collisional tectonics, extensional collapse and lateral escape of fragments of the Adriatic (Apulian) plate and their complex interaction with the European foreland in the Tertiary (e.g. Royden et al. 1982; Mahel' 1986; Csontos 1995; Ratschbacher et al. 1991; Tari et al. 1992; Plašienka 1996, 1997; Frisch et al. 2000; Sperner et al. 2002). Although orogen dynamics in the case of the Western Carpathians is well described by conceptual models (see e.g. Kováč et al. 1994; Plašienka et al. 1997a), important aspects, such as the timing and grade of metamorphism or the timing and rate of exhumation and topography formation, are little understood or controversial. This is due to lack of empirical data and a sparse geological record.

In this study, we focus on the Nízke Tatry Mts. (NT; Lower Tatra Mountains in English) in the central part of the Western Carpathians (Fig. 1a), a key area for understanding the Alpine history of the region. Tectonothermal evolution of the NT is believed to be well understood (e.g. Kováč et al. 1994), but, this understanding is not supported by empirical data. Furthermore, inferring from our experiences in other mountain ranges in the Western Carpathians we suspect that some classic models and long accepted definitions might be misconceptions:

1. Similar to other 'core' mountains in the Western Carpathians (i.e. basement-cored mountains belonging to the Tatric superunit sensu Mahel' 1986 and Plašienka et al. 1997a), the core of the NT is comprised of Variscan crystalline basement consisting of Variscan granitoids and metamorphic rocks. In Carpathian literature, the Tatric Variscan basement complexes including the NT are traditionally defined as completely lacking or being only weakly overprinted by an Alpine metamorphic event. Traditionally, the Alpine overprint is thought to be restricted to narrow shear zones, reaching P–T conditions of the anchizone or lower greenschist facies (Bujnovský and Lukáčik 1985; Krist et al. 1992; Plašienka et al. 1997a; Madarás et al. 1996; Plašienka 2003a, b). However, based on petrographical and thermochronological evidence, this widely accepted definition was challenged by some authors who argued that some Variscan granitic cores did experience very low-grade (anchizonal) Alpine metamorphic overprint (Faryad and Dianiška 2002; Danišík et al. 2008a, 2010).
2. The generally accepted model of exhumation for the Western Carpathians was presented by Kováč et al. (1994). Based on AFT data, the authors proposed a progressive exhumation of crystalline bodies, migrating from internal parts of the belt towards the orogenic front, with the NT being exhumed in the Eocene (37–52 Ma). Recently, work on other 'core' mountains has implied that this model is imprecise (Danišík et al. 2004, 2008a, 2010), however, no new data from the NT have as yet been reported.
3. The NT form an E–W oriented ridge, about 70 km long, 20–30 km wide, >2,000 m high (Fig. 1b), which is the second highest ridge in the Western Carpathians. It represents the most important watershed in the Western Carpathians, but its topographic evolution is poorly understood. In the Pleistocene, the topography of the NT was probably fairly similar to that of the present, dictating the pattern of local mountain glaciation (Louček et al. 1960), but the question of when the present-day high relief formed has not been addressed.

To tackle these issues, samples from a transect across the NT ridge were analyzed using a combination of four thermochronometers: zircon fission track (ZFT), zircon (U–Th)/He (ZHe), apatite fission track (AFT) and apatite (U–Th–[Sm])/He (AHe) dating methods. Sensitivities of these methods cover the temperature range of ~270–40°C (Hurford 1986; Wagner and Van den haute 1992; Brandon et al. 1998; Wolf et al. 1998; Carlson et al. 1999; Farley 2000). The multi-dating approach facilitates a reconstruction of the full thermal evolution at mid- to shallow crustal levels and addresses the issues of metamorphism, burial and exhumation, and topographic evolution raised above.

2 Geological setting

In this study we focus on the western part of the NT, which is dominated by Variscan crystalline basement with sparsely preserved Mesozoic sedimentary cover and two Mesozoic superficial nappes (Fatric and Hronic, respectively) flanking the basement on the north and south (Fig. 1c, d).

The basement consists of Variscan granitoids (zircon U/Pb ages: 343 ± 4 and 330 ± 10 Ma; Poller et al. 2001; Putiš et al. 2003) and Variscan metamorphic rocks (mostly

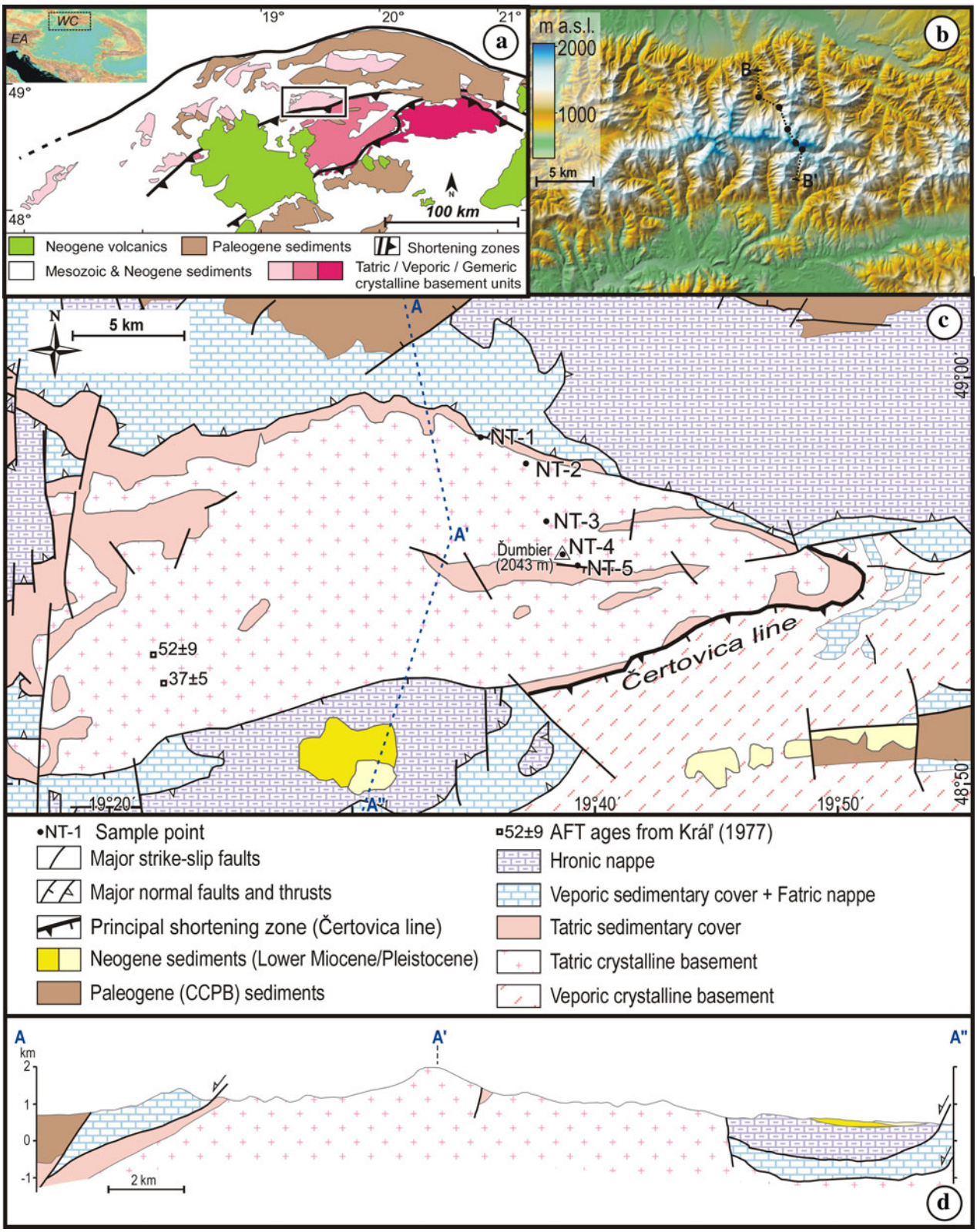

Fig. 1 **a** Tectonic sketch map of the Western Carpathians with exposures of Variscan crystalline complexes belonging to three principal units and occurrences of Paleogene sediments and Neogene volcanic rocks. *Inset map* shows the location **a**; *WC* Western Carpathians, *EA* Eastern Alps. **b** Digital elevation model of the Nízke Tatry Mts. (NT) with position of the samples and trace of the profile presented in the Fig. 2. **c** Geological sketch map of the NT and surrounding areas (modified after Biely et al. 1992; Lexa et al. 2000) with location of the samples and AFT ages reported by Kráľ (1977). **d** Schematic profile after Biely et al. (1992) (for location, see *dashed line* in **b**)

amphibolite-facies paragneiss, orthogneiss, amphibolite and migmatite; U/Pb ages ~360 Ma; e.g. Putiš et al. 2009a). Variscan cooling of the basement is constrained by K/Ar and Ar/Ar dating of muscovite and biotite (ages ~330–300 Ma; Kantor et al. 1984; Maluski et al. 1993; Dallmeyer et al. 1996). The studied area is classified in the Carpathian literature as a part of the Tatric superunit (or Tatricum; Mahel' 1986; Plašienka et al. 1997a) and according to the traditional definition, as the part of the Tatricum, the basement should lack an Alpine metamorphic overprint (Mahel' 1986; Plašienka et al. 1997a). To the southeast, the Tatric basement is bordered by a distinct thrust zone (Čertovica line) composed of mylonitic and phyllonitic rocks (Biely and Fusán 1969). This thrust zone separates Tatric basement and cover in the footwall from a hanging wall basement unit (Veporicum) in the southeast and is considered one of the most important Alpine shortening zones in the Western Carpathians (Biely and Fusán 1969; Plašienka et al. 1997b). Although the age of activity of the Čertovica line has not been radiometrically determined, it is accepted that thrusting of basement units and emplacement of superficial nappes occurred during the Alpine (Eo-Alpine) collision between the European and the Adriatic plate from ~110 to ~85 Ma. This has been inferred from paleontological evidence from the nappe sequences, and both K/Ar and Ar/Ar data from similar shear zones (e.g. Dallmeyer et al. 1996; Plašienka 1997; Putiš et al. 2009a).

Post-thrusting evolution of the NT remains unclear because there are no post-Cretaceous sediments preserved directly on the basement of the NT, but it can be traced in the sedimentary record of the surrounding depressions (Fig. 1c, d). The first post-Cretaceous record is represented by deposits of the Central Carpathian Palaeogene Basin (CCPB) preserved north and south of the range (Fig. 1c, d; Gross 1978; Gross 2008; Gross et al. 1984). The CCPB sediments reach a thickness of up to 3.5–4 km in the deepest part of the basin (Soták 1998; Janočko and Jacko 2001) and consist of shallow to deep marine sediments of Lutetian to Aquitanian age (Gross et al. 1984; Gross 2008). On the northern slopes of the NT, thickness of these clastic and organo-detritic sediments reaches 500–600 m and increases towards the north, reaching a maximum of 1,600 m (Gross et al. 1980). South of the NT, a maximum of 550 m is reached (Filo in Bezák et al. 2009). It is noteworthy that clastic material from the NT crystalline basement was found in CCPB sequences on both sides of the NT mountains ridge. The position of the NT during the CCPB sedimentation is controversial. Gross et al. (1984) and Gross (2008) argued that the crystalline basement was eroded and has supplied material to the CCPB since the Late Eocene (~36 Ma), whereas Kázmér et al. (2003) argued for a burial of the NT by CCPB sediments from the Middle to Late Eocene (~40–38 Ma) until the Late Oligocene (~28 Ma).

Occurrences of Neogene sediments can be found only south of the range and are represented by Oligocene(?)–Lower Miocene conglomerates, consisting of pebbles of dolomites, limestones and the crystalline basement (Biely and Samuel 1982). It is widely accepted that during Neogene times, the NT were subjected to erosion and karstification but did not yet form a pronounced mountain range as there are no post-Lower Miocene sediments preserved in the area (Biely et al. 1992; Kováč 2000 and references therein). The mountain range must have existed in the Pleistocene as evidenced by the presence of glaciers at that time (Louček et al. 1960).

The exhumation history of the NT has been investigated by means of thermochronology by Král' (1977). The author reported two AFT ages (52 ± 9 and 37 ± 5 Ma) measured by the now obsolete population dating method and argued for Eocene uplift although no track length data justifying this statement were provided. This conclusion was then widely accepted by the geological community and has served as the main support for the currently accepted exhumation model for the Western Carpathians (Kováč et al. 1994).

3 Samples and methods

Five samples of the Variscan granite were collected for thermochronological investigation from a tectonically undisturbed, ~8 km long profile, crossing the ridge of the NT through the highest peak (Figs. 1b, c, 2a). The maximum vertical difference between the samples is 887 m; sample NT-1 was taken from the tectonic contact of the basement and Triassic limestone, representing the basal part of the Fatric nappe thrust upon the crystalline basement in the Turonian (Biely et al. 1992); sample NT-4 was taken from the highest peak of the NT (Ďumbier, 2,045 m a.s.l.).

Apatite and zircon grains were separated using conventional magnetic and heavy liquid separation techniques. Fission track analysis was carried out using standard procedures described in Danišík et al. (2007). The external detector method (Gleadow 1981) was applied with the etching protocols of Donelick et al. (1999) for apatite (5.5 M HNO_3 for 20 s at 21°C) and Zaun and Wagner (1985) for zircon (eutectic mixture of KOH and NaOH at 215°C for 12 h). The zeta calibration approach (Hurford and Green 1983) was adopted to determine the ages. FT ages were calculated using TrackKey 4.2 g (Dunkl 2002). In apatite, horizontal confined tracks in tracks were measured in c-axis parallel surfaces and were normalized for crystallographic angle using a c-axis projection (Donelick et al. 1999; Ketcham et al. 2007a). The annealing properties of apatite were assessed by measuring Dpar values (Dpar, the mean etch pit diameter of fission tracks measured on the apatite polished surface parallel to the crystallographic c-axis; e.g. Burtner et al. 1994).

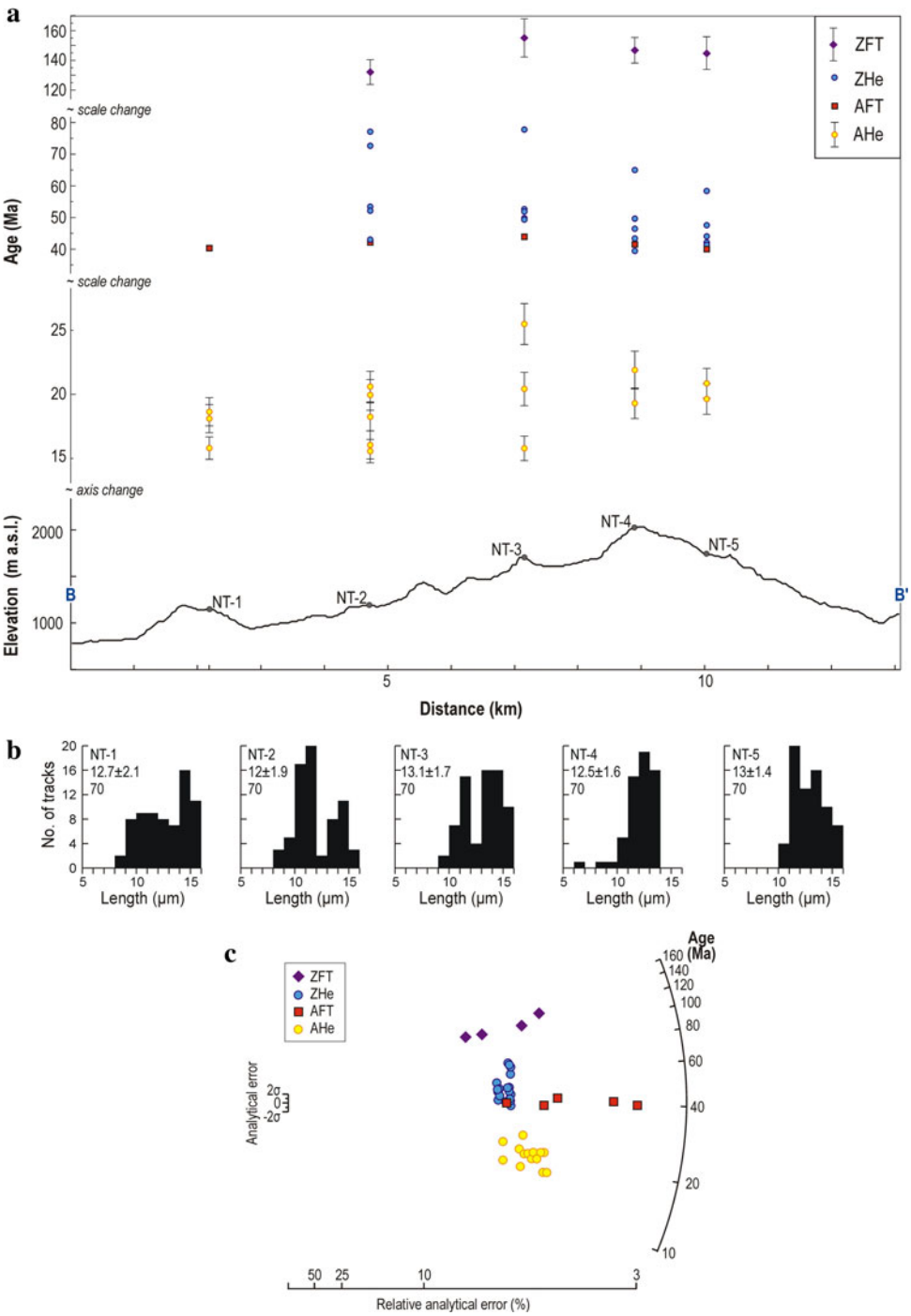

Fig. 2 **a** Topographic profile with position of the samples and measured thermochronological data. *AFT* apatite fission track, *AHe* apatite (U–Th–[Sm])/He, *ZFT* zircon fission track, *ZHe* zircon (U–Th)/He. Large spread of AHe ages hampers any attempts of correlation with topography. **b** Apatite fission track length data. Explanation in histograms (from *top*): sample code; mean track length ± SD (both in μm); number of measured tracks. **c** All data displayed on a radial plot (Galbraith 1988; Vermeesch 2009), clearly showing minimum difference between AFT and ZHe ages, pointing to a fast cooling in the Eocene. ZFT and AHe form well separated clusters related to different thermal events

For (U–Th–[Sm])/He analysis, apatite and zircon crystals were hand-picked following strict selection criteria (Farley 2002; Reiners 2005), then photographed and measured. Apatite was loaded in Pt tubes, degassed at ~960°C under vacuum using laser-heating or furnace and analyzed for ^{4}He using a Pfeiffer Prisma QMS-200 mass spectrometer. Following He measurements, the apatite was spiked with ^{233}U and ^{230}Th, dissolved in nitric acid and analyzed by isotope dilution inductively coupled mass spectrometry for U, Th and in one batch also for Sm on a Perkin Elmer (ELAN DRC II) ICP-MS. Zircon was loaded in Nb tubes, degassed at ~1,250°C and analyzed for ^{4}He using the same facility as for apatite. Degassed zircon was dissolved following the procedure of Evans et al. (2005) and analyzed by isotope dilution inductively coupled mass spectrometry for U and Th on an Agilent 7500 ICP-MS. For more details on analytical procedures, the reader is referred to Evans et al. (2005) and Danišík et al. (2008c).

Total analytical uncertainty was calculated as the square root of the sum of the squares of weighted uncertainties on U, Th, Sm and He measurements. Total analytical uncertainty was less than ~5% in all cases and was used to calculate the error of raw (U–Th–[Sm])/He ages. The raw AHe and ZHe ages were corrected for alpha ejection (Ft correction) after Farley et al. (1996) and Hourigan et al. (2005), respectively. A value of 5% was adopted as the uncertainty on the Ft correction, and was used to calculate errors for the corrected AHe and ZHe ages.

The low-temperature thermal history based on fission track and (U–Th–[Sm])/He data was modelled using the HeFTy modelling program (Ketcham 2005) operated with the multikinetic fission track annealing model of Ketcham et al. (2007b) and the diffusion kinetics of the Durango apatite after Farley (2000) and zircon after Reiners et al. (2004). Inferring from fission track mounts, we assumed homogeneous distribution of U and Th in the apatite and zircon.

4 Results

The results of thermochronological analyses are summarized in Tables 1 and 2 and shown in Fig. 2. All five samples yielded fairly consistent results, clearly defining distinct age groups. Higher temperature chronometers revealed older ages than chronometers with lower temperature sensitivity, which is in agreement with the closure temperature concept (Dodson 1973).

ZFT age spectra are fairly broad, but passed the Chi-square test and thus represent a single age population. The ZFT ages form a loose cluster of Late Jurassic–Early Cretaceous age (132.1 ± 8.3; 155.1 ± 12.9; 146.8 ± 8.6; 144.9 ± 11.0 Ma).

ZHe data ages reproduce well: in most of the cases four out of five replicates reproduce within one sigma error and one replicate is a 'flier' considerably older than the rest. Single grain ZHe ages of reproducible replicates form a tight cluster of Early–Middle Eocene age ranging from 53.4 ± 3.8 to 39.4 ± 2.6 Ma (15 replicates). The 'fliers' range from 77.8 ± 5.2 to 58.3 ± 4.1 Ma (5 replicates). AFT ages are slightly younger than ZHe ages and form a distinct cluster of Middle Eocene age (40.3 ± 1.7; 42.1 ± 1.9; 43.9 ± 2.4; 41.5 ± 2.8; 40.0 ± 2.3 Ma; Fig. 2a, c), indicating rapid cooling through the zircon ZHe partial retention zone (~200–160°C; Reiners et al. 2004) and apatite partial annealing zone (~120–60°C; Wagner and Van den haute 1992) during that period. All AFT samples passed the Chi-square test and are therefore considered to form one age population. The average Dpar value for all samples is ~1.6 µm, indicating fluorine-rich apatite, characterized by relatively low annealing temperature (~60–120°C; e.g. Wagner and Van den haute 1992; Ketcham et al. 1999). Four of five track length distributions are bimodal, with short mean track lengths (MTL 12.0–13.1 µm) and relatively large standard deviations (Fig. 2b), pointing to a complex thermal evolution with a long residence or a phase of reheating within the apatite partial annealing zone (Gleadow et al. 1986a, b).

Due to the unacceptable quality of apatite grains for purposes of (U–Th–[Sm])/He dating and frequent occurrence of fluid and mineral inclusions, we could not always measure five replicates per sample as in the case of zircon. The presence of microscopically undetected inclusions became obvious after the second gas extraction (so called 're-extract'). In such cases we did not proceed with U–Th measurements but rather tried to select another crystal. Despite significant effort, in only one sample (NT-2) were five replicates successfully measured, whereas the rest of the samples were run in duplicate and triplicate. Nevertheless, AHe ages are consistent, with the majority clustering around the Early Miocene. This suggests a Miocene residence of the samples within AHe partial retention zone and corroborates the assumption of complex cooling or reheating inferred from the track length distributions.

We found no obvious correlation between thermochronological data and sample elevation (Fig. 2a), suggesting that all samples experienced a fairly similar cooling history.

5 Interpretation and discussion

5.1 Alpine metamorphism

The Late Jurassic–Early Cretaceous ZFT ages show that the NT basement must have reached temperatures >210°C during post-Variscan times (assuming an effective closure temperature of 240 ± 30°C; Brandon et al. 1998) as the 'Variscan memory' in the ZFT system was fully reset. The maximum temperature must have been lower than ~300°C, since the Ar/Ar system retains Variscan ages (Maluski et al. 1993; closure temperature of Ar/Ar system in biotite is ~300°C; Harrison et al. 1985; McDougall and Harrison 1988). Given these constraints, the basement must have experienced a very low-grade or low-grade Alpine metamorphic overprint, in contrast to the traditionally accepted notion of no overprint (see Sect. 2; Mahel' 1986; Plašienka et al. 1997a). These data thus clearly prove a very low-grade (anchizonal) Alpine overprint in the Tatric superunit (Faryad and Dianiška 2002; Danišík et al. 2008a, 2010).

Although the presence of Alpine metamorphism is documented by the ZFT data, its timing and geodynamic

Table 1 Fission track results

Sample code	Lat. WGS-84	Lon.	Elev. (m a.s.l.)	Lithology	N	ρ_s	N_s	ρ_i	N_i	ρ_d	N_d	P(χ^2) (%)	Age (Ma)	$\pm1\sigma$ (Ma)	MTL (μm)	SD (μm)	N (L)	Dpar (μm)
AFT data																		
NT-1	48.9813	19.5840	1,156	Granite	25	9.436	1,206	24.051	3,074	6.255	5,426	69	40.3	1.7	12.7	2.1	70	1.6
NT-2	48.9716	19.6153	1,200	Granite	20	16.916	977	39.927	2,306	6.052	5,426	>95	42.1	1.9	12.0	1.9	70	1.6
NT-3	48.9496	19.6282	1,700	Granite	20	10.613	614	25.669	1,485	6.457	5,426	84	43.9	2.4	13.1	1.7	70	1.6
NT-4	48.9363	19.6401	2,043	Granite	20	3.824	359	9.277	871	6.119	5,426	>95	41.5	2.8	12.5	1.6	70	1.6
NT-5	48.9300	19.6510	1,750	Granite	20	5.145	532	12.640	1,307	5.984	5,426	>95	40.0	2.3	13.0	1.4	70	1.6
ZFT data																		
NT-2z	48.9716	19.6153	1,200	Granite	25	191.115	1,304	57.159	390	6.459	3,089	>95	132.1	8.3				
NT-3z	48.9496	19.6282	1,700	Granite	20	202.393	778	52.029	200	6.530	3,089	>95	155.1	12.9				
NT-4z	48.9363	19.6401	2,043	Granite	30	190.123	1,754	51.162	472	6.479	3,089	48	146.8	8.6				
NT-5z	48.9300	19.6510	1,750	Granite	20	173.430	900	47.982	249	6.561	3,089	>95	144.9	11.0				

Ages were calculated using zeta calibration method (Hurford and Green 1983), glass dosimeters CN-5 and CN-2 (for apatites and zircons, respectively), and zeta values of 329.8 ± 7.1 (apatite) and 123.6 ± 2.1 year/cm^2 (zircon)

N number of dated apatite crystals, ρ_s (ρ_i) spontaneous (induced) track densities ($\times10^5$ tracks/cm^2), N_s (N_i) number of counted spontaneous (induced) tracks, ρ_d dosimeter track density ($\times10^5$ tracks/cm^2), N_d number of tracks counted on dosimeter; $P(\chi^2)$ probability obtaining Chi-square value (χ^2) for n degree of freedom (where n = no. of crystals − 1), $Age \pm 1\sigma$ central FT age ± 1 standard error (Galbraith and Laslett 1993), *MTL* mean track length, *SD* standard deviation of track length distribution, *N(L)* number of horizontal confined tracks measured, *Dpar* average etch pit diameter of fission tracks, *AFT* apatite fission track, *ZFT* zircon fission track

Table 2 (U–Th–[Sm])/He results

Sample code	N_c	Th (ng)	Th error (%)	U (ng)	U error (%)	Sm (ng)	Sm error (%)	He (ncc)	He error (%)	TAU (%)	Th/U	Unc. age (Ma)	$\pm 1\sigma$ (Ma)	F_t	Cor. age (Ma)	$\pm 1\sigma$ (Ma)
Apatite																
NT-1#1	1	0.139	2.4	0.244	0.2	1.296	5.8	0.417	0.9	2.4	0.56	11.9	0.3	0.75	15.8	0.9
NT-1#2	1	0.077	2.5	0.207	1.9	1.110	6.1	0.373	0.9	2.4	0.37	13.1	0.3	0.72	18.1	1.1
NT-1#3	1	0.138	2.4	0.234	1.9	1.491	5.6	0.453	0.9	2.4	0.59	13.4	0.3	0.72	18.6	1.1
Central age (Ma) ± SD (Ma)															17.5 ± 1.5	
NT-2#0	2	0.132	1.1	0.286	1.7	N/a	n/a	0.443	2.6	3.1	0.46	11.5	0.4	0.74	15.6	0.9
NT-2#1	1	0.137	1.5	0.166	1.2	n/a	n/a	0.284	4.5	4.7	0.82	11.8	0.6	0.73	16.1	1.1
NT-2#2	1	0.015	2.9	0.186	1.9	0.417	5.6	0.294	0.9	2.3	0.08	12.5	0.3	0.61	20.6	1.2
NT-2#3	1	0.014	2.9	0.140	2.0	0.378	5.9	0.230	0.9	2.4	0.10	12.9	0.3	0.65	20.0	1.2
NT-2#4	1	0.017	2.8	0.251	1.9	0.757	5.7	0.390	0.9	2.2	0.07	12.3	0.3	0.67	18.2	1.1
Central age (Ma) ± SD (Ma)															18.0 ± 2.2	
NT-3#1	1	0.028	2.7	0.071	2.6	0.442	5.6	0.158	0.9	2.9	0.38	15.9	0.6	0.62	25.5	1.6
NT-3#2	1	0.016	2.9	0.054	3.2	0.395	5.5	0.076	0.9	3.4	0.30	10.2	0.4	0.65	15.8	1.0
NT-3#3	1	0.019	2.8	0.056	3.0	0.405	5.7	0.107	0.9	3.3	0.34	13.8	0.5	0.68	20.4	1.3
Central age (Ma) ± SD (Ma)															20.2 ± 4.9	
NT-4#1	1	0.017	2.9	0.031	4.5	0.127	6.0	0.068	0.9	4.5	0.55	15.4	0.7	0.71	21.9	1.5
NT-4#2	1	0.017	2.9	0.041	3.5	0.139	5.6	0.074	0.9	3.6	0.42	13.1	0.5	0.68	19.3	1.2
Central age (Ma) ± SD (Ma)															20.6 ± 1.8	
NT-5#1	1	0.043	2.6	0.185	1.9	1.034	5.5	0.362	0.9	2.4	0.23	14.6	0.5	0.70	20.9	1.2
NT-5#2	1	0.021	2.8	0.118	2.1	1.193	5.7	0.236	0.9	2.7	0.18	14.7	0.6	0.75	19.6	1.2
Central age (Ma) ± SD (Ma)															20.2 ± 0.7	
Zircon																
NT-2#1*	1	0.875	5.3	4.884	4.3	n/a	n/a	36.589	0.5	4.4	0.18	58.8	2.6	0.81	72.6	4.8
NT-2#2	1	1.207	5.3	5.339	4.3	n/a	n/a	29.953	0.5	4.4	0.23	43.6	1.9	0.84	52.1	3.5
NT-2#3*	1	1.270	5.3	3.467	4.3	n/a	n/a	30.424	0.5	4.4	0.37	66.1	2.9	0.86	77.1	5.1
NT-2#4	1	0.596	4.6	1.336	4.8	n/a	n/a	8.177	1.2	4.9	0.45	45.4	2.2	0.85	53.4	3.8
NT-2#5	1	0.557	4.5	0.820	4.8	n/a	n/a	3.985	1.2	4.9	0.68	34.4	1.7	0.80	43.0	3.0
Central age (Ma) ± SD (Ma) (all replicates)															58.2 ± 14.5	
Central age (Ma) ± SD (Ma) (fliers omitted)															49.3 ± 5.7	
NT-3#1	1	0.895	5.3	2.486	4.3	n/a	n/a	14.666	0.5	4.4	0.36	44.6	2.0	0.85	52.6	3.5
NT-3#2*	1	1.822	5.3	4.074	4.3	n/a	n/a	36.657	0.6	4.4	0.45	66.6	2.9	0.86	77.8	5.2
NT-3#3	1	1.273	5.3	4.871	4.3	n/a	n/a	26.945	0.5	4.4	0.26	42.7	1.9	0.86	49.8	3.3
NT-3#4	1	0.232	4.4	1.917	4.8	n/a	n/a	10.273	1.2	4.9	0.12	42.7	2.1	0.87	49.4	3.5
NT-3#5	1	0.274	4.4	0.822	4.8	n/a	n/a	4.832	0.9	4.8	0.33	44.6	2.2	0.86	51.9	3.6
Central age (Ma) ± SD (Ma) (all replicates)															55.4 ± 12.1	
Central age (Ma) ± SD (Ma) (fliers omitted)															50.9 ± 1.6	
NT-4#1	1	0.278	5.3	4.580	4.3	n/a	n/a	15.118	0.5	4.3	0.06	26.7	1.2	0.68	39.4	2.6
NT-4#2	1	0.638	5.3	6.505	4.3	n/a	n/a	23.758	0.5	4.4	0.10	29.3	1.3	0.68	43.3	2.9
NT-4#3	1	0.034	4.8	0.669	4.8	n/a	n/a	2.919	0.9	4.9	0.05	35.3	1.7	0.76	46.4	3.2
NT-4#4*	1	0.465	5.3	3.097	4.3	n/a	n/a	20.458	0.5	4.4	0.15	52.2	2.3	0.80	65.0	4.3
NT-4#5	1	0.206	4.7	1.755	4.9	n/a	n/a	7.845	0.9	4.9	0.12	35.7	1.8	0.72	49.6	3.5
Central age (Ma) ± SD (Ma) (all replicates)															48.0 ± 9.8	
Central age (Ma) ± SD (Ma) (fliers omitted)															44.5 ± 4.3	
NT-5#1	1	0.583	5.3	6.019	4.3	n/a	n/a	24.474	0.5	4.3	0.10	32.6	1.4	0.77	42.1	2.8
NT-5#2	1	0.656	5.3	7.432	4.3	n/a	n/a	36.121	0.5	4.4	0.09	39.0	1.7	0.82	47.6	3.2
NT-5#3	1	0.639	5.3	3.162	4.3	n/a	n/a	13.000	0.5	4.4	0.20	32.2	1.4	0.78	41.4	2.7

Table 2 continued

Sample code	N_c	Th (ng)	Th error (%)	U (ng)	U error (%)	Sm (ng)	Sm error (%)	He (ncc)	He error (%)	TAU (%)	Th/U	Unc. age (Ma)	$\pm 1\sigma$ (Ma)	F_t	Cor. age (Ma)	$\pm 1\sigma$ (Ma)
NT-5#4*	1	0.079	4.6	0.706	4.9	n/a	n/a	4.343	0.9	5.0	0.11	49.0	2.4	0.84	58.3	4.1
NT-5#5	1	0.113	4.4	0.634	4.8	n/a	n/a	2.733	0.9	4.9	0.18	33.9	1.7	0.77	44.0	3.1
Central age (Ma) ± SD (Ma) (all replicates)															46.3 ± 6.9	
Central age (Ma) ± SD (Ma) (fliers omitted)															43.7 ± 2.8	

Aliquots NT-2#0 and NT-2#1 were He extracted by furnace, the rest by laser. Samples marked with asterisk are considered as 'fliers'

N_c number of dated crystals, *Th* ^{232}Th, *U* ^{238}U, *Sm* ^{147}Sm, *He* ^{4}He at STP, *TAU* total analytical uncertainty, *Unc. age* uncorrected He age, *Ft* alpha recoil correction factor after Farley et al. (1996) an Hourigan et al. (2005), *Cor. age* corrected He age

context remains uncertain. This is because no track lengths in zircons were measured and the thermal history could not be modelled, thus the meaning of the data is less clear. From the perspective of regional geology it is important to note that similar Jurassic to Early Cretaceous ZFT ages have been found in other parts of the Western Carpathians (Kováč et al. 1994; Plašienka et al. 2007). Furthermore, Danišík et al. (2010) reported almost identical Late Jurassic–Early Cretaceous ZFT ages from an adjacent Tatric crystalline basement (Malá Fatra Mts.) that should have had a common evolution to the NT throughout the Mesozoic (Plašienka et al. 1997a). The authors provide an extensive discussion of the possible meaning of these ZFT ages and we speculate that the ZFT ages are either (1) cooling ages recording a Jurassic/Cretaceous thermal event, perhaps related to the rifting (Plašienka 2003b; Putiš et al. 2009b) associated with increased heat flow and magmatic activity (Hovorka and Spišiak 1988; Spišiak and Hovorka 1997; Spišiak and Balogh 2002) or (2) apparent ages resulting from partial rejuvenation of the ZFT system during the Eo-Alpine collision (~110–85 Ma; Danišík et al. 2010).

5.2 Eocene exhumation

A tight cluster of Early–Middle Eocene ZHe ages and Middle Eocene AFT ages, backed up by the thermal modelling results (see Sect. 5.3) give strong evidence for a rapid cooling event between ~50 and ~40 Ma, when the NT basement cooled from ZHe partial retention zone to apatite partial annealing zone. Exhumation rates between 50 and 40 Ma determined by the mineral pair method and by conversion of modelled trajectories are in the range of ~250–900 m/Ma (assuming a geothermal gradient of 30°C/km; closure temperatures of ~190 and ~110°C for ZHe and AFT system, respectively; Reiners et al. 2004; Wagner and Van den haute 1992).

We interpret the cooling event as being related to collapse of the Carpathian orogenic wedge and explain it as follows: during the Eo-Alpine collision in the mid-Cretaceous, the Tatric superunit was overthrust by superficial nappes and its interior, including the NT crystalline core, was perhaps partly overridden by the Veporic basement/cover complex. This compressional event is well documented in the stratigraphy and by Ar/Ar ages from shear zones ranging between ~100 and 85 Ma (Dallmeyer et al. 1996; Putiš et al. 2009a). As a result of thrusting, the NT basement must have been buried to depths where the temperature was elevated enough to fully reset the ZHe system (>190°C) and even partially reset the ZFT system (>210°C).

The Eocene cooling so well documented by ZHe and AFT data is most likely related to exhumation of the NT basement, pointing to an extensional collapse of the Carpathian orogenic wedge during the Eocene. Although predominantly erosion-driven exhumation can be inferred from extensive occurrences of upper Middle to Upper Eocene detritus from the NT in the surrounding depressions, relatively high cooling rates are difficult to explain solely by erosion. Thus, we speculate that the exhumation could have an important tectonic component. Several studies have mentioned that in the Tertiary, the Čertovica line was reactivated as a transtensional or extensional shear zone (e.g. Šefara et al. 1998; Plašienka 2003a; Putiš et al. 2009a). It is likely that this process tectonically exhumed the footwall Tatric basement from below the hanging wall Veporic basement sheet.

5.3 Post-Eocene thermal event?

The post-tectonic evolution of the NT is difficult to track from the limited geological record, so the Miocene AHe ages may represent an important contribution to this topic. In order to elucidate the meaning of the AHe data, we first review relevant facts and currently accepted models, which we then test by thermal modelling, before presenting our conclusion.

Bartonian to Rupelian flysch sediments of the CCPB basin gave rise to two different models for the Palaeogene period (for current distribution of CCPB sediments see Fig. 1a):

1. Gross et al. (1984) and Gross (1978, 2008) suggest that already in the early Middle Eocene (Lutetian), prior to sedimentation of CCPB, the emerged NT formed a

topographic high which was prone to erosion and was never covered by Palaeogene sediments. The first CCPB sediments of Bartonian age were derived from the Mesozoic cover nappes and Tatric sedimentary cover. Crystalline basement was first eroded and supplied material to the CCPB at the Bartonian/Priabonian boundary (~37 Ma), as documented by submarine fan deposits with crystalline clasts preserved north of the range. Material supply from the NT, however, quickly ceased by the Priabonian, as inferred from transport direction as well as lithological data. Nevertheless, the NT should have formed an island in the Palaeogene sea during Priabonian–Rupelian times (Gross 2008).

2. Kázmér et al. (2003), in contrast, proposed a large scale model for the Eastern Alps and Western Carpathians, whereby, from Bartonian to Egerian times (~40–28 Ma), the NT were completely buried by a thick pile of CCPB sediments.

Neogene tectonothermal history is even more difficult to track. Given the lack of sediments, it is widely accepted that the NT were not affected by Neogene transgression (Kováč 2000), so no reheating induced by burial should be expected. On the other hand, several studies have shown that the Tatric crystalline complexes were affected by a Miocene regional thermal event related to increased heat flow and volcanic activity in the Western Carpathian region (Danišík et al. 2008a, b; for current distribution of Neogene volcanic rocks see Fig. 1a).

In order to test these hypotheses, we used the HeFTy modelling program (Ketcham 2005) to calculate thermal histories that reconcile ZHe, AFT and AHe data. According to the hypotheses presented above, we tested four plausible cooling scenarios: simple cooling in the Eocene (after Gross 2008), Palaeogene burial (after Kázmér et al. 2003), Miocene reheating (after Danišík et al. 2008a, b), and superimposed Palaeogene burial and Miocene reheating (after Kázmér et al. 2003; Danišík et al. 2008a, b combined).

We found that the thermal trajectories, which best reconcile the measured data as given by the highest 'goodness of fit' values, are characterized by a fast cooling from >190 to <60°C at ~55–40 Ma, and require a reheating to ~55–90°C before cooling to the present-day temperature conditions (Fig. 3a–d). While the interpretation of the fast cooling is straight forward in terms of post-collisional

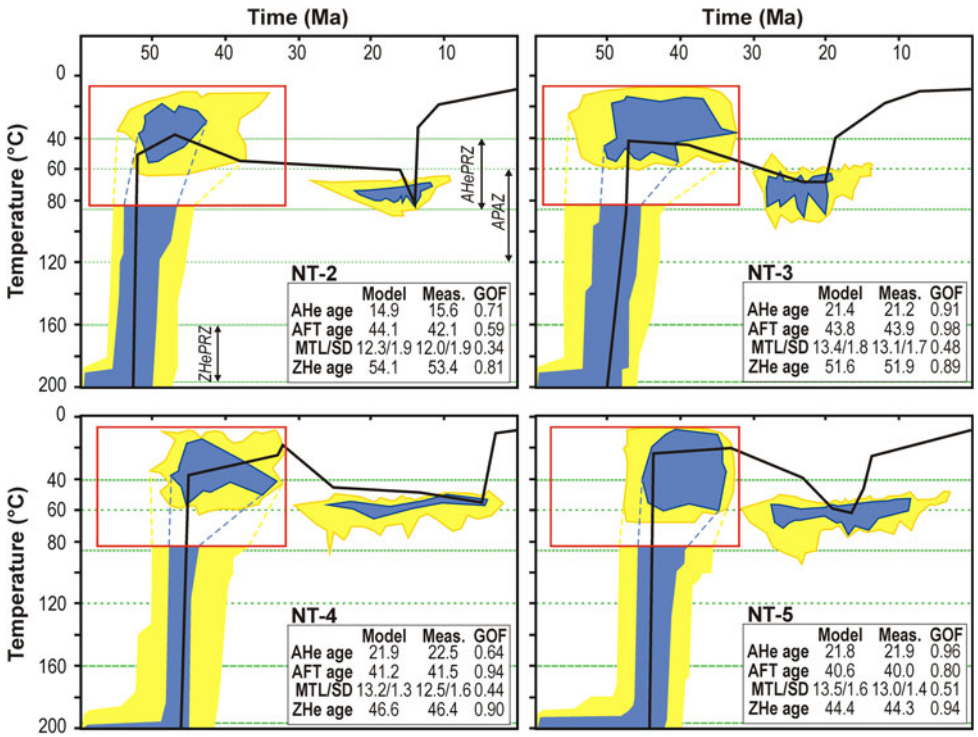

Fig. 3 Thermal modelling results of thermochronological data displayed in a time–temperature diagram modelled with the HeFTy program (Ketcham, 2005). The best fit is shown as a *solid black line*, shaded polygons (*yellow* acceptable fit, *blue* good fit) show the values of peak temperatures after Eocene cooling and during post-Eocene reheating. *ZHePRZ* ZHe partial retention zone, *APAZ* apatite partial annealing zone, *AHePRZ* AHe partial retention zone, *MTL* mean track length in µm, *SD* standard deviation in µm, *GOF* goodness of fit (statistical comparison of the measured input data and modelled output data, where a "good" result corresponds to value 0.5 or higher, "best" result corresponds to value 1). Note that according to the modelling results, reheating could occur anytime from the Oligocene to the Late Miocene and thus is not in favour of any of the suggested geological scenarios

collapse and exhumation, the meaning of the reheating episode is ambiguous. Unfortunately, the modelling could not resolve exactly when the heating pulse occurred and the suggested time span of 30–5 Ma is too broad to favour any of the above-mentioned scenarios. The only conclusion which can be drawn with confidence from the modelling results is that the NT must have experienced a thermal event between ~30 and 5 Ma with minimum peak temperatures of ~55–90°C. This event could be related either to the CCPB burial in the Oligocene or magmatic activity in the Miocene or Miocene sedimentary burial, where all options are equally plausible given the lack of geological constraints and considering the modelling results only. Nevertheless, inferring from the Early Miocene AHe age cluster, we are inclined to prefer a Miocene thermal event, related to magmatic activity and/or sedimentary burial.

5.4 Failed approach to palaeo-topography reconstruction

One of the objectives of this study was to obtain a better understanding of the topographic evolution of the NT. Our strategy was based on AHe dating of a ridge-valley profile crossing the NT ridge in the highest point. According to theory, the spatial pattern of AHe ages should reflect the amount of erosion or the shape of the subsurface isotherms, thereby providing constraints on palaeotopography and its change through time (Reiners 2007).

Despite demonstrated feasibility by several studies (e.g. House et al. 1998, 2001; Foeken et al. 2007), in our case this approach failed for two reasons: Firstly, the key requirement of this approach is that AHe ages are cooling ages, which allow straightforward calculation of erosion. Here, however, as proven by modelling results, AHe ages are not cooling ages related to a distinct cooling event, but are apparent ages resulting from a complex thermal history with a phase of reheating. In addition, we do not even know when this reheating occurred or its duration. Secondly, the resolution of the AHe dataset is too low (or the spread of single grain AHe ages is too high) to be correlated with present day topography (Fig. 2c). This is probably a consequence of a combination of several factors such as complex thermal history, quality of dated apatite grains, less pronounced relief (with too short wavelength and too low amplitude), or slow exhumation rates during the post-collisional stage. Therefore, we cannot draw any conclusion on the palaeotopographic evolution of the NT from our AHe data.

6 Conclusions

New ZFT, ZHe, AFT and AHe data enabled us to constrain the thermotectonic evolution of the NT and provide important constraints on the thermal and geodynamic evolution of the Western Carpathians. The most important results can be summarized as follows:

- The Variscan crystalline basement of the NT was heated to temperatures above ~210°C and experienced a very low-grade to low-grade Alpine metamorphic overprint as documented by the Late Jurassic–Early Cretaceous ZFT ages ranging from 155.1 ± 12.9 to 132.1 ± 8.3 Ma. The timing and source of the heating remain unclear. We propose two alternative explanations: (1) either the ZFT ages are cooling ages related to a Jurassic/Cretaceous thermal event or (2) ZFT ages are apparent ages resulting from a partially reset during Eo-Alpine collision and thrusting in the mid-Cretaceous. Despite this ambiguity, ZFT data clearly disprove the widely accepted notion of non-existent Alpine metamorphism in the crystalline core complexes of the Tatric superunit.
- ZHe and AFT data constrain a distinct fast cooling event in the Eocene between ~55 and 40 Ma, which we interpret in terms of erosional and tectonic exhumation of the basement, related to the collapse of the Carpathian orogenic wedge. This is the first thermochronological evidence univocally documenting cooling of the Tatric crystalline core in the Eocene.
- AHe data revealed a thermal event in the Oligocene–Miocene, when the crystalline basement was heated to temperatures of ~55–90°C. Given the lack of geological information and insufficient resolution of the modelling results, this thermal event may be related to Oligocene/Miocene sedimentary burial, Miocene mantle upwelling, magmatic activity and/or increased heat flow in the Carpathian realm. Regardless of the cause, this finding disproves the widely accepted concept of thermal stability of the NT during the post-Eocene period.
- Complex thermal evolution resulting in apparent AHe ages and limited resolution of thermochronological data did not allow us to place solid constraints on the topographic evolution of the NT.

Acknowledgments This study was financed by the German Science Foundation. We thank C. Scadding and A. Thomas (TSW Analytical) for assistance with ICP MS. The sampling campaign was supported by the Grant Agency of the Academy of Sciences, Czech Republic (# A3013201) and by the Institute of Geology, v.v.i., Academy of Sciences of the Czech Republic (#AV0Z30130516). An earlier version of the manuscript benefited from constructive reviews by C. Persano, L. Fodor, B. Fügenschuh and an anonymous reviewer.

References

Bezák, V., Biely, A., Broska, I., Bóna, J., Buček, S., Elečko, M., Filo, I., Fordinál, K., Gazdačko, L'., Grecula, P., Hraško, L'.,

Ivanička, J., Jacko, S. sen., Jacko, S. jun., Janočko, J., Kaličiak, M., Kobulský, J., Kohút, M., Konečný, V., Kováčik, M. (Bratislava), Kováčik, M. (Košice), Lexa, J., Madarás, J., Maglay, J., Mello, J., Nagy, A., Németh, Z., Olšavský, M., Plašienka, D., Polák, M., Potfaj, M., Pristaš, J., Siman, P., Šimon, L., Teťák, F., Vozárová, A., Vozár, J., & Žec, B. (2009). . Bratislava: Dionýz Štúr Publish*Explanation to general geological map of the Slovak Republic 1:200 000*ing House (in Slovak, with English summary).

Biely, A., & Samuel, O. (1982). On the question of the red Vajsková Conglomerate in the Lopej Basin. *Geologické Práce, Správy, 77*, 103–110. (in Slovak).

Biely, A., Beňuška, P., Bezák, V., Bujnovský, A., Halouzka, R., Ivanička, J., et al. (1992). *Geological map of the Nízke Tatry Mountains, 1:50, 000*. Bratislava: Dionýz Štúr Publishing house. (in Slovak, with English summary).

Biely, D., & Fusán, O. (1969). Zum Problem der Wurzelzonen der subtatrischen Decken. *Geologické Práce, Správy, 42*, 51–64.

Brandon, M. T., Roden-Tice, M. K., & Garver, J. I. (1998). Late Cenozoic exhumation of the Cascadia accretionary wedge in the Olympic Mountains, NW Washington State. *Geological Society of America Bulletin, 110*(8), 985–1009.

Bujnovský, A., & Lukáčik, E. (1985). Geology of NW parts of Nízke Tatry Mts. and adjacent part of the Vel'ká Fatra Mts. *Západné Karpaty, Geológia, 10*, 39–65. (in Slovak, with English summary).

Burtner, R. L., Nigrini, A., & Donelick, R. A. (1994). Thermochronology of Lower Cretaceous source rocks in the Idaho-Wyoming thrust belt. *American Association of Petroleum Geologists Bulletin, 78*(10), 1613–1636.

Carlson, W. D., Donelick, R. A., & Kecham, R. A. (1999). Variability of apatite fission-track annealing kinetics: I. Experimental results. *American Mineralogist, 84*, 1213–1223.

Csontos, L. (1995). Tertiary tectonic evolution of the Intra-Carpathian area: A review. *Acta Vulcanologica, 7*, 1–13.

Dallmeyer, R. D., Neubauer, F., Handler, R., Fritz, H., Müller, W., Pana, D., & Putiš, M. (1996). Tectonothermal evolution of the internal Alps and Carpathians: Evidence from $^{40}Ar/^{39}Ar$ mineral and whole-rock data. *Eclogae Geologicae Helvetiae, 89*, 203–227.

Danišík, M., Dunkl, I., Putiš, M., Frisch, W., & Král', J. (2004). Tertiary burial and exhumation history of basement highs along the NW margin of the Pannonian Basin—an apatite fission track study. *Austrian Journal of Earth Sciences, 95*(96), 60–70.

Danišík, M., Kohút, M., Broska, I., & Frisch, W. (2010). Thermal evolution of the Malá Fatra Mountains (Central Western Carpathians): insights from zircon and apatite fission track thermochronology. *Geologica Carpathica, 61*(1), 19–27.

Danišík, M., Kohút, M., Dunkl, I., & Frisch, W. (2008a). Thermal evolution of the Žiar Mountains basement (Inner Western Carpathians, Slovakia) constrained by fission track data. *Geologica Carpathica, 59*(1), 19–30.

Danišík, M., Kohút, M., Dunkl, I., Hraško, L'., & Frisch, W. (2008b). Apatite fission track and (U–Th)/He thermochronology of the Rochovce granite (Slovakia)—implications for thermal evolution of the Western Carpathians-Pannonian region. *Swiss Journal of Geosciences, 101*(1), 225–233.

Danišík, M., Kuhlemann, J., Dunkl, I., Székely, B., & Frisch, W. (2007). Burial and exhumation of Corsica (France) in the light of fission track data. *Tectonics, 26*, TC1001. doi:10.1029/2005TC001938.

Danišík, M., Sachsenhofer, R. F., Privalov, V. A., Panova, E. A., Frisch, W., & Spiegel, C. (2008c). Low-temperature thermal evolution of the Azov Massif (Ukrainian Shield–Ukraine)—implications for interpreting (U–Th)/He and fission track ages from cratons. *Tectonophysics, 456*, 171–179.

Dodson, M. H. (1973). Closure temperatures in cooling geochronological and petrological systems. *Contributions to Mineralogy and Petrology, 40*, 259–274.

Donelick, R. A., Ketcham, R. A., & Carlson, W. D. (1999). Variability of apatite fission-track annealing kinetics: I. Experimental results. *American Mineralogist, 84*(9), 1224–1234.

Dunkl, I. (2002). TRACKKEY: A Windows program for calculation and graphical presentation of fission track data. *Computers and Geosciences, 28*(2), 3–12.

Evans, N. J., Byrne, J. P., Keegan, J. T., & Dotter, L. E. (2005). Determination of uranium and thorium in zircon, apatite, and fluorite: Application to laser (U–Th)/He thermochronology. *Journal of Analytical Chemistry, 60*(12), 1159–1165.

Farley, K. A. (2000). Helium diffusion from apatite: general behavior as illustrated by Durango fluorapatite. *Journal of Geophysical Research, 105/B2*, 2903–2914.

Farley, K. A. (2002). (U–Th)/He dating: techniques, calibrations, and applications. *Reviews in Mineralogy and Geochemistry, 47*, 819–844.

Farley, K. A., Wolf, R. A., & Silver, L. T. (1996). The effect of long alpha-stopping distances on (U–Th)/He ages. *Geochimica et Cosmochimica Acta, 60*(21), 4223–4229.

Faryad, S. W., & Dianiška, I. (2002). Ti-bearing andradite-prehnite-epidote assemblage from the Malá Fatra granodiorite and tonalite (Western Carpathians). *Schweizerische Mineralogische und Petrogrologische Mitteilungen, 83*, 47–56.

Foeken, J. P. T., Persano, C., Stuart, F. M., & ter Voorde, M. (2007). Role of topography in isotherm perturbation: apatite (U–Th)/He and fission track results from the Malta tunnel, Tauern Window, Austria. *Tectonics, 26*. doi:10.1029/2006TC002049.

Frisch, W., Dunkl, I., & Kuhlemann, J. (2000). Post-collisional large-scale extension in the Eastern Alps. *Tectonophysics, 327*, 239–265.

Galbraith, R. F. (1988). Graphical display of estimates having differing standard errors. *Technometrics, 30*, 271–281.

Galbraith, R. F., & Laslett, G. M. (1993). Statistical models for mixed fission track ages. *Nuclear Tracks and Radiation Measurements, 21*, 459–470.

Gleadow, A. J. W. (1981). Fission-track dating methods: What are the real alternatives? *Nuclear Tracks and Radiation Measurements, 5*(1/2), 3–14.

Gleadow, A. J. W., Duddy, I. R., & Green, P. F. (1986a). Fission track lengths in the apatite annealing zone and the interpretation of mixed ages. *Earth and Planetary Science Letters, 78*, 245–254.

Gleadow, A. J. W., Duddy, I. R., & Green, P. F. (1986b). Confined fission track lengths in apatite: a diagnostic tool for thermal history analysis. *Contributions to Mineralogy and Petrology, 94*, 405–415.

Gross, P. (1978). Paleogene beneath Central-Slovakian neovolvanic rocks (in Slovak). In J. Vozár (Ed.), *Paleogeographical evolution of the Western Carpathians* (pp. 121–145). Bratislava: Dionýz Štúr Institute of Geology.

Gross, P. (2008). *Litostratigraphy of the Western Carpathians: Paleogene–Podtatranská Group*. Bratislava: Dionýz Štúr Publishing house. (in Slovak, with English summary).

Gross, P., Köhler, E., Biely, A., Franko, O., Hanzel, V., Hricko, J., et al. (1980). *Gology of the Liptovská kotlina Depression*. Bratislava: Dionýz Štúr Publishing House. (in Slovak, with English summary).

Gross, P., Köhler, E., & Samuel, O. (1984). New lithostratigraphic classification of the Central Carpathians Paleogene. *Geologické Práce, Správy, 81*, 103–117. (in Slovak).

Harrison, T. M., Duncan, I., & McDougall, I. (1985). Diffusion of ^{40}Ar in biotite: Temperature, pressure and compositional effects. *Geochimica et Cosmochimica Acta, 49*(11), 2461–2468.

Hourigan, J. K., Reiners, P. W., & Brandon, M. T. (2005). U-Th zonation-dependent alpha-ejection in (U–Th)/He chronometry. *Geochimica et Cosmochimica Acta, 69*, 3349–3365.

House, M. A., Wernicke, B. P., & Farley, K. A. (1998). Dating topography of the Sierra Nevada, California, using apatite (U–Th)/He ages. *Nature, 396*, 66–69.

House, M. A., Wernicke, B. P., & Farley, K. A. (2001). Paleogeomorphology of the Sierra Nevada, California, from (U–Th)/He ages in apatite. *American Journal of Science, 301*, 77–102.

Hovorka, D., & Spišiak, J. (1988). *Mesozoic volcanism of the Western Carpathians*. Bratislava: Veda Publishing House. (in Slovak, English summary).

Hurford, A. J. (1986). Cooling and uplift patterns in the Lepontine Alps South Central Switzerland and age of vertical movement on the Insubric fault line. *Contributions to Mineralogy and Petrology, 92*, 413–427.

Hurford, A. J., & Green, P. F. (1983). The zeta age calibration of fission-track dating. *Chemical Geology, 41*, 285–312.

Janočko, J., & Jacko, S. (2001). Turbidite Deposit Systems of the Central-Carpathian Paloegene Basin. *Geolines, 13*, 133–140.

Kantor, J., Repčok, I., Ďurkovičová, J., Elias, K., & Wiegerová, V. (1984). *The time evolution of selected areas from the Western Carpathians according radiometric dating*. Open file report. Bratislava: Geofond (in Slovak).

Kázmér, M., Dunkl, I., Frisch, W., Kuhlemann, J., & Ozsvárt, P. (2003). The Palaeogene forearc basin of the Eastern Alps and the Western Carpathians: Subduction erosion and basin evolution. *Journal of the Geological Society, London, 160*, 413–428.

Ketcham, R. A. (2005). Forward and inverse modeling of low-temperature thermochronometry data. In P. W. Reiners & T. A. Ehlers (Eds.), *Low-Temperature Thermochronology: Techniques, Interpretations, and Applications* (pp. 275–314). Reviews in Mineralogy and Geochemistry 58.

Ketcham, R. A., Carter, A., Donelick, R. A., Barbarand, J., & Hurford, A. J. (2007a). Improved modeling of fission-track annealing in apatite. *American Mineralogist, 92*, 789–798.

Ketcham, R. A., Carter, A., Donelick, R. A., Barbarand, J., & Hurford, A. J. (2007b). Improved modeling of fission-track annealing in apatite. *American Mineralogist, 92*, 799–810.

Ketcham, R. A., Donelick, R. A., & Carlson, W. D. (1999). Variability of apatite fission track annealing kinetics: III. Extrapolation to geologic time scales. *American Mineralogist, 84*, 1235–1255.

Kováč, M. (2000). *Geodynamic, paleogeographical and structural evolution of the Carpathian—Pannonian realm in the Miocene: A new view on the Neogene basins of Slovakia*. Bratislava: Veda. (in Slovak).

Kováč, M., Král', J., Márton, E., Plašienka, D., & Uher, P. (1994). Alpine uplift history of the Central Western Carpathians: geochronological, paleomagnetic, sedimentary and structural data. *Geologica Carpathica, 45*, 83–96.

Král', J. (1977). Fission track ages of apatites from some granitoid rocks in West Carpathians. *Geologický Zborník—Geologica Carpathica, 28*, 269–276.

Krist, E., Korikovsky, S. P., Putiš, M., Janák, M., & Faryad, S. W. (1992). *Geology and petrology of metamorphic rocks of the Western Carpathian crystalline complexes*. Bratislava: Comenius University Press.

Lexa, J., Bezák, V., Elečko, M., Eliáš, M., Konečný, V., Less, Gy., et al. (2000). *Geological map of Western Carpathians and adjacent areas 1: 500, 000*. Bratislava: Ministry of the Environment of Slovak Republic Geological Survey of Slovak Republic.

Louček, D., Michovská, J., & Trefná, E. (1960). Glaciation of the Low Tatra Mountains. *Sborník Československé společnosti zeměpisné, 65*(4), 326–352. (In Czech, with English summary).

Madarás, J., Hók, J., Siman, P., Bezák, V., Ledru, P., & Lexa, O. (1996). Extension tectonics and exhumation of crystalline basement of the Veporicum unit (Central Western Carpathians). *Slovak Geological Magazine, 3–4*, 179–183.

Mahel', M. (1986). *Geological structure of the Czechoslovak Carpathians*. Bratislava: Veda Publishing House. (in Slovak).

Maluski, H., Rajlich, P., & Matte, P. (1993). $^{40}Ar/^{39}Ar$ dating of the Inner Carpathians Variscan basement and Alpine mylonitic overprint. *Tectonophysics, 223*, 313–337.

McDougall, I., & Harrison, T. M. (1988). *Geochronology and thermochronology by the $^{40}Ar/^{39}Ar$ method*. New York: Oxford University Press.

Plašienka, D. (1996). Mid-Cretaceous (120–80 Ma) orogenic process in the Central Western Carpathians. Brief review and interpretation of data. *Slovak Geological Magazine, 3–4*(96), 319–324.

Plašienka, D. (1997). Cretaceous tectonochronology of the Central Western Carpathians (Slovakia). *Geologica Carpathica, 48*, 99–111.

Plašienka, D. (2003a). Development of basement-involved fold and thrust structures exemplified by the Tatric–Fatric–Veporic nappe system of the Western Carpathians (Slovakia). *Geodinamica Acta, 16*, 21–38.

Plašienka, D. (2003b). Dynamics of Mesozoic pre-orogenic rifting in the Western Carpathians. *Mitteilungen der Österreichischen Geologischen Gesellschaft, 93*, 79–98.

Plašienka, D., Broska, I., Kissová, D., & Dunkl, I. (2007). Zircon fission-track dating of granites from the Vepor-Gemer Belt (Western Carpathians): constraints for the Early Alpine exhumation history. *Journal of GEOsciences, 52*, 113–123.

Plašienka, D., Grecula, P., Putiš, M., Kováč, M., & Hovorka, D. (1997a). Evolution and structure of the Western Carpathians: an overview. In P. Grecula, D. Hovorka, & M. Putiš (Eds.), *Geological evolution of the Western Carpathians* (pp. 1–24). Mineralia Slovaca, Monograph, Bratislava.

Plašienka, D., Putiš, M., Kováč, M., Šefara, J., & Hrušecký, I. (1997b). Zones of Alpidic subduction and crustal underthrusting in the Western Carpathians. In P. Grecula, D. Hovorka, & M. Putiš (Eds.), *Geological evolution of the Western Carpathians* (pp. 35–42). Mineralia Slovaca, Monograph, Bratislava.

Poller, U., Todt, W., Kohút, M., & Janák, M. (2001). Nd, Sr, Pb isotope study of the Western Carpathians: Implications for Palaeozoic evolution. *Schweitzerische Mineralogische Pertrographische Mitteilungen, 81*(2), 159–174.

Putiš, M., Frank, W., Plašienka, D., Siman, P., Sulák, M., & Biroň, A. (2009a). Progradation of the Alpidic Central Western Carpathians orogenic wedge related to two subductions: Constrained by $^{40}Ar/^{39}Ar$ ages of white micas. *Geodinamica Acta, 22*(1–2), 55–80.

Putiš, M., Ivan, P., Kohút, M., Spišiak, J., Siman, P., Radvanec, M., et al. (2009b). Meta-igneous rocks of the West-Carpathians basement as an indicator of Early Paleozoic extension-rifting/breakup events. *Bulletin de la Societé Géologique de France, 180*(6), 461–471.

Putiš, M., Kotov, A. B., Petrík, I., Korikovsky, S. P., Madarás, J., Salnikova, E. B., et al. (2003). Early- vs. Late orogenic granitoids relationships in the Variscan basement of the Western Carpathians. *Geologica Carpathica, 54*, 163–174.

Ratschbacher, L., Frisch, W., Linzer, H.-G., & Merle, O. (1991). Lateral extrusion in the eastern Alps, 2, Structural analysis. *Tectonics, 10*, 257–271.

Reiners, P. W. (2005). Zircon (U-Th)/He Thermochronometry. In P. W. Reiners & T. A. Ehlers (Eds.), *Low-Temperature Thermochronology: Techniques, Interpretations, and Applications* (pp. 151–176). Reviews in Mineralogy and Geochemistry 58.

Reiners, P. W. (2007). Thermochronologic approaches to paleotopography. *Reviews in Mineralogy and Geochemistry, 66*, 243–267.

Reiners, P. W., Spell, T. L., Nicolescu, S., & Zanetti, K. A. (2004). Zircon (U-Th)/He thermochronometry: He diffusion and comparisons with $^{40}Ar/^{39}Ar$ dating. *Geochimica et Cosmochimica Acta, 68*, 1857–1887.

Royden, L. H., Horváth, F., & Burchfiel, B. C. (1982). Transform faulting, extension, and subduction in the Carpathian Pannonian region. *Geological Society of America Bulletin, 93*, 717–725.

Šefara, J., Kováč, M., Plašienka, D., & Šujan, M. (1998). Seismogenic zones in the Eastern Alpine-Western Carpathian-Pannonian junction area. *Geologica Carpathica, 49*, 247–260.

Soták, J. (1998). Sequence stratigraphy approach to the Central Carpathian Paleogene (Eastern Slovakia): eustasy and tectonics as controls of deep-sea fan deposition. *Slovak Geological Magazine, 4*, 185–190.

Sperner, B., Ratschbacher, L., & Nemčok, M. (2002). Interplay between subduction retreat and lateral extrusion: Tectonics of the Western Carpathians. *Tectonics, 21*, 1–24.

Spišiak, J., & Balogh, K. (2002). Mesozoic alkali lamprophyres in Variscan granitoids of the Malé Karpaty and Nízke Tatry Mountains—geochronology and geochemistry. *Geologica Carpathica, 53*, 295–301.

Spišiak, J., & Hovorka, D. (1997). Petrology of the Western Carpathians Cretaceous primitive alkaline volcanics. *Geologica Carpathica, 48*, 113–121.

Tari, G., Horváth, F., & Rumpler, J. (1992). Styles of extension in the Pannonian Basin. *Tectonophysics, 208*, 203–219.

Vermeesch, P. (2009). RadialPlotter: A Java application for fission track, luminescence and other radial plots. *Radiation Measurements, 44*(4), 409–410.

Wagner, G. A., & Van den haute, P. (1992). *Fission-track dating*. Stuttgart: Enke Verlag.

Wolf, R. A., Farley, K. A., & Kass, D. M. (1998). Modeling of the temperature sensitivity of the apatite (U–Th)/He thermochronometer. *Chemical Geology, 148*, 105–114.

Zaun, P., & Wagner, G. A. (1985). Fission track stability in zircon under geological conditions. *Nuclear Tracks and Radiation Measurements, 10*, 303–307.